

Chaos and irreversibility in simple model systems

Wm. G. Hoover

Department of Applied Science, University of California at Davis/Livermore and Lawrence Livermore National Laboratory, Livermore, California 94551-7808

Harald A. Posch

Institute for Experimental Physics, University of Vienna, Boltzmannngasse 5, Vienna A-1090, Austria

(Received 24 November 1997; accepted for publication 27 February 1998)

The multifractal link between chaotic time-reversible mechanics and thermodynamic irreversibility is illustrated for three simple chaotic model systems: the Baker Map, the Galton Board, and many-body color conductivity. By scaling time, or the momenta, or the driving forces, it can be shown that the dissipative nature of the three thermostated model systems has analogs in conservative Hamiltonian and Lagrangian mechanics. Links between the microscopic nonequilibrium Lyapunov spectra and macroscopic thermodynamic dissipation are also pointed out.

© 1998 American Institute of Physics. [S1054-1500(98)01102-1]

Atomistic simulations of macroscopic irreversible processes require a generalization of the usual Newtonian mechanics. One approach incorporates nonequilibrium constraints into the equations of motion. An alternative approach couples a Newtonian system to one or more heat reservoirs. Both atomistic approaches lead to fractal descriptions quite unlike Gibbs' continuous probability densities. The fractals reflect the rarity of nonequilibrium states relative to the equilibrium ones. We illustrate the formation of such fractal structures for a series of simple models. In order of increasing complexity—and realism—these are (i) a mapping of the unit square onto itself, (ii) the one-body dynamics of a particle driven through an array of fixed scatterers by an external field, and (iii) the many-body dynamics of a fluid with a field driving half the particles to the right and half to the left. The two last dynamical models illustrate that the fractal structures characterizing constrained systems have analogs describing driven systems. The many-body fluid exhibits macroscopic chaotic modes, analogous to hydrodynamic modes, associated with the individual instabilities described by the Lyapunov exponents.

I. INTRODUCTION

The subject of this meeting at Eötvös University, "Chaos and Irreversibility," emphasizes the link between time-reversible, chaotic microscopic mechanics and irreversible macroscopic dissipation. The main idea is to examine the basic principles underlying the simulation and analysis of thermodynamic and hydrodynamic processes. This subject was popularized by Boltzmann, as described in the lecture by E. G. D. Cohen. Boltzmann's explanation of macroscopic irreversibility, in isolated dilute gases, was statistical, based on the one-particle distribution function.

Seventy-five years later, at the Livermore and Los Alamos laboratories, fast computers opened the door to a revolutionary possibility—the study of irreversible processes from detailed dynamical many-body trajectories.¹ Distribu-

tion functions could be accumulated, by time averaging, but were no longer the fundamental ingredient for theoretical understanding. By 1972 nonequilibrium many-body simulations had suggested a new path to understanding irreversibility,^{2,3} and presently led to the discovery of multifractal phase-space structures, in 1986.^{4,5} Now, 100 years after Boltzmann, simulations with 10^7 particles are feasible.⁶

Recent conceptual advances, resulting from few-body and many-body simulations, were discussed here in Budapest, in 1997. The new multifractal structures, which provide an explanation for irreversibility, followed from three independent theoretical approaches, discussed here in the lectures by Dorfman and Gaspard. All three are tied closely to the solution of chaotic nonlinear problems using traditional classical mechanics. Assimilation of this explanation and understanding has been delayed, for about ten years, by a disparity in viewpoint. For those that view computers as tools for simulation and numerical solution, it is natural to stress trajectory-based dynamics as fundamental. Boltzmann and Gibbs' statistical heritage suggests instead that a statistical distribution-based dynamics could be considered fundamental. In addition to this dichotomy, to which we return later, there is also a point of view that the puzzling aspects of irreversibility are solely due to the chosen initial conditions.⁷ Chaos seems to us to have made this last point of view outdated.

The multifractal structures generated by dynamical nonequilibrium many-body simulations describe what is often called the "natural measure" of the dynamics, a record of the relative probabilities of visiting neighborhoods of particular state points. Such a measure can be represented by point sets of coordinates $\{q(ndt)\}$, which could be further idealized as defining continuous differentiable trajectories $\{q(t)\}$. Alternatively, the same trajectories could be given a phase-space representation: $\{q(t), p(t)\}$. So as to emphasize parallels with Boltzmann's gas theory, and Gibbs' statistical mechanics, we adopt this last representation. The "multifractal" character implies that the singular nature of the points' density in phase space, $f(q, p)$, varies from point to point. At

an arbitrary point (q_0, p_0) the number of nearby $\{q, p\}$ trajectory points within a generalized distance δr varies as a fractional "fractal" power of δr . Because this exponent depends upon the location (q_0, p_0) the underlying phase-space structure is termed "multifractal" rather than just fractal. Though the characterization of nonequilibrium phase-space attractors, in geometric or topological terms, is far from complete, rudimentary properties, such as the information dimension, the average value of the power-law exponent, are directly related to macroscopic observables, such as the external entropy production.⁸

Away from equilibrium, time-reversible dynamics, with either "flows" (sets of ordinary differential equations) or "maps" (explicit equations linking the dependent variables at successive times) giving the evolution, leads naturally to the creation of Lyapunov-unstable repeller-attractor pairs in phase space,^{4,5} with the flow, or the mapping, proceeding from the repeller (upon which the comoving volume expands) to the attractor (upon which the volume shrinks). Surprisingly, the low-dimensional flows which can be investigated exhaustively, with computer graphics, are typically "ergodic," with any trajectory repeatedly coming arbitrarily close to any allowed point in the phase space.^{9,10} The "repeller" acts as the source of such a flow. This repeller is a time-reversed image of its more-stable cousin, the "strange attractor," so that the two share exactly the same fractal dimensionality. The repeller has a positive Lyapunov-exponent sum, indicating an inherent instability, occupation of a growing region in phase space, while the attractor has the negative exponent sum corresponding to dissipation and collapse. The natural measures of the repeller and attractor correspond to phase volumes of reduced dimensionality, not just reduced size. Thus the rarity of nonequilibrium states is qualitative, not just quantitative.⁴

The dynamics is "time-reversible." Any time-reversed trajectory $\{q(-t), -p(-t)\}$ is a perfectly valid solution of the motion equations, with the momentum variables and the time changed in sign. Paradoxically, the sign of the summed Lyapunov spectrum, which must be negative for stability, changes sign too.¹¹ This paradoxical sign change signals that reversed nonequilibrium trajectories are actually not observable, and correspond to repeller states even less stable than the observed states found on the attractor. This conclusion is the mechanical analog of the second law of thermodynamics.⁴

Assimilating the concepts and ideas involved in this relatively new understanding of irreversibility can be expedited by the dynamical study of simple example problems. In this summary introduction to the subject we outline three examples, (i) a simple two-dimensional map,¹² (ii) a continuous flow,^{8,9} confined to a three-dimensional hypersurface in a four-dimensional phase space, and (iii) a many-body problem in a phase space with dimensionality just under 500 000.¹³ The three examples are chaotic and time-reversible. They have multifractal solutions and so exhibit macroscopic irreversibility. We begin by describing the details of these systems; then we discuss the general features of dynamical simulations of their behavior; we then use this picture of what is known to predict the unknown: what re-

mains to be accomplished in the near future. It is prudent to keep in mind, throughout, that micromechanics and irreversible continuum mechanics are conceptually different. The macroscopic approach contains no thermal fluctuations and no way of recalling the past. For these reasons there is a limit to the correspondence which can be drawn between them. In reality the two views are separated by a logical gulf, just as physics is separated from biology and economics.

II. TIME-REVERSIBLE DISSIPATIVE BAKER MAP

Maps, which take one phase-space point into another, are simpler than flows, and this motivates their study. While the jumping action of the one-dimensional logistic map can show "chaos" (Lyapunov instability), continuous flows require at least three dimensions, just to avoid the periodicity which must result whenever a deterministic trajectory crosses itself. But maps share enough common features with flows to make their study worthwhile, particularly if understanding the related flows is complicated. Because our multifractal understanding of irreversibility is not entirely complete, maps provide useful insight. It appears that a particularly useful property of such maps, to assure their relevance to flows, is time reversibility. For physicists, time reversibility is usually thought of in a way more restrictive than the definition used in the mathematical literature. We call a map, or a flow, "time reversible" if a sequence of points generated by it corresponds to a series of time-reversed points (in which some of the variables may change sign), generated by exactly the same map, or flow, using the final condition (with any necessary sign changes) as the starting condition of the reversed sequence.

The simplest time-reversible map, which has also the chaotic and irreversible properties important for this meeting, is a rotated version of the "Baker Map," generalized so that area is not preserved locally. In the case considered here comoving areas are either doubled or halved with an iteration of the map. This generalized Baker Map is defined by Fig. 1. It is easy to confirm that the map is time-reversible. It operates in a square domain, with the coordinate origin, $(q, p) = (0, 0)$, at the center of the square. A typical point (q, p) , within the square, is mapped to a new point:

$$(q, p) \rightarrow (q', p'),$$

as is illustrated in Fig. 1. Time reversibility corresponds to the same mapping's carrying that time-reversed point $(q', -p')$ to the time-reversed initial point:

$$(q', -p') \rightarrow (q, -p).$$

The figure also shows 100 000 points generated by iteration of this map. The "ergodicity" of the mapping is suggested by the figure, ergodicity means approaching arbitrarily close to any given point in the domain. Because the mapping gives a spreading parallel to lines of constant $q + p$ the distribution in that direction is essentially random. Thus local values of the Lyapunov exponents, λ_1 and λ_2 , can be estimated: because the probability of undergoing twofold expansion [with local exponents $\ln(3/1)$ and $\ln(2/3)$] is $1/3$,

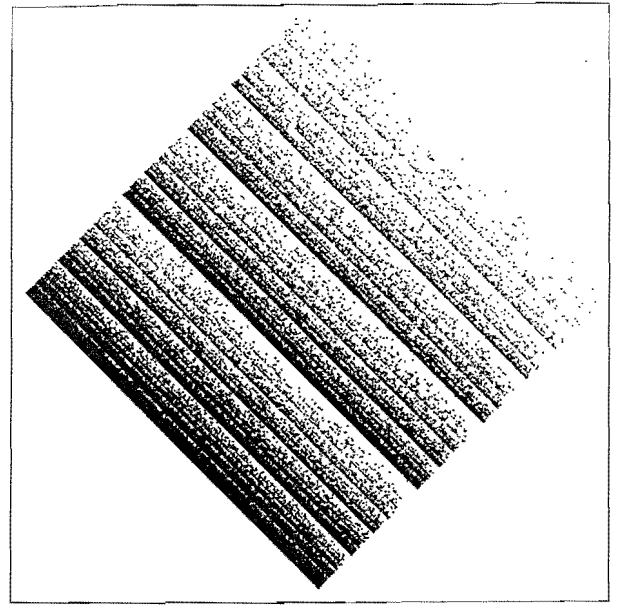
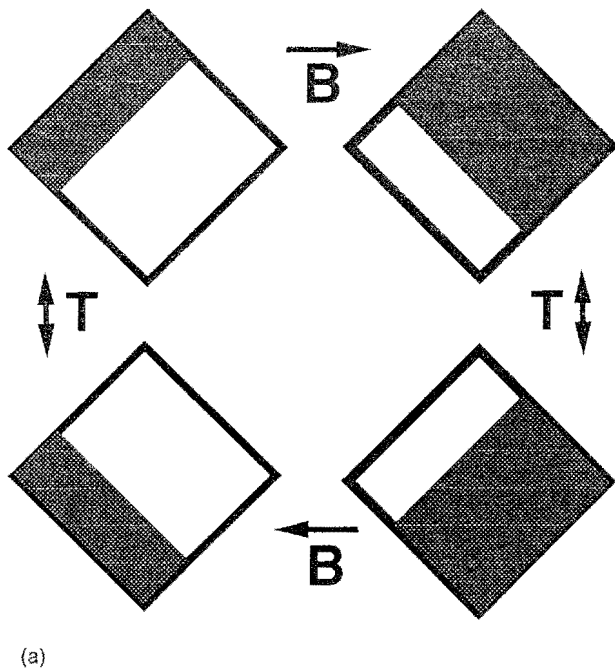


FIG. 1. Time-reversible dissipative Baker Map. The basic mapping process "B" stretches without rotation, and is shown at the left. "T" indicates time-reversal, changing the sign of the vertical coordinate. When the Baker map is applied to the initial point (0.1,0.1), it generates the attractor shown at the right. Of the 100 000 points shown, 66 490 lie in the largest of the self-similar regions. Using the first 10 000 000 points gave 6 666 340 points in this region, in good agreement with the "random" expectation, $2N/3$.

while the probability of undergoing twofold compression [with local exponents $\ln(3/2)$ and $\ln(1/3)$] is $2/3$, the time-averaged exponents are

$$\lambda_1 = (1/3)\ln(27/4), \quad \lambda_2 = (1/3)\ln(2/27).$$

The Kaplan-Yorke dimension of the attractor shown in Fig. 1, the dimension of an object which neither grows nor shrinks in the long term, is also the information dimension:¹⁴

$$D_{KY} = D_I = 1 + (\lambda_1 / |\lambda_2|) = 1.734.$$

The paradoxical qualities of a time-reversible strange attractor are present here. The long-term change in a small comoving phase volume \otimes , following the "motion" through N iterations, is negative, approaching zero as the iteration number N increases:

$$\begin{aligned} \langle \otimes_N / \otimes_0 \rangle &= \left\langle \prod (\otimes_n / \otimes_{n-1}) \right\rangle \\ &\doteq e^{N(\lambda_1 + \lambda_2)} \doteq (2/1)^{N/3} \times (1/2)^{2N/3}. \end{aligned}$$

Likewise paradoxically, the probability density increases toward infinity, on average,

$$\begin{aligned} \langle f_N / f_0 \rangle &= \left\langle \prod (f_n / f_{n-1}) \right\rangle \\ &\doteq e^{-N(\lambda_1 + \lambda_2)} \doteq (2/1)^{2N/3} \times (1/2)^{N/3}. \end{aligned}$$

This odd behavior is generic for nonequilibrium time-reversible stationary states.^{4,15} "Stationary" is a euphemism for time-independent, and refers to the motion equations and the imposed boundary conditions, both are here defined by the map.

We stress that stationarity is a property of the dynamics, rather than the solution, because the form of the solution continually changes, showing more and more detail with iteration, on finer and finer scales, $\propto t^{-1/2}$, as the time t progresses and more data are generated. From the mathematical point of view, repellers and attractors are limiting stationary sets, for infinitely long sampling times. From the computational point of view, any numerical approximation to these structures continues to develop in time, and never achieves stationarity. Though both the repeller and the attractor have negligible measure in the usual sense, being fractal objects with dimensionality 1.734 in this illustrative case, the flow condenses onto the attractor with probability one. This simple condensation process, onto a zero-volume fractal set, is the microscopic mechanical analog of the second law of thermodynamics.^{4,15} Although fluctuations can occur (corresponding to a run of phase-volume increases, with corresponding decreases in f) it is obvious that, eventually, the second law (corresponding to overall volume decrease and the divergence of f) must be satisfied. No other stationary time-development can be consistent with a bounded phase volume.

It might be thought that the finite precision, typically eight figures, of computer simulations would spoil the generality of the conclusions. But simulations using double or quadruple precision indicate that there is no noticeable effect of increased accuracy. In this connection Levesque and Verlet have shown how to generate a perfectly reversible equilibrium dynamics by using integer coordinates.^{16,17} It has been stated that a "coarse-graining" is essential to an understanding of nonequilibrium dynamics.^{18,19} That is, the devel-

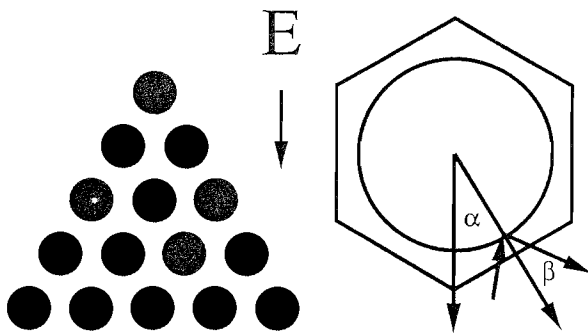


FIG. 2. Galton Board. An abridged 15-scatterer portion of the structure is shown at the left. The full Galton Board can be represented computationally by the reduced dynamics within a single cell, as is shown at the right. The angles α and β describe the location and post-collision velocity direction, for each scattering.

oping multifractal structure of the phase-space density must be ignored, below some usually unspecified scale. As Tél has emphasized, there are advantages in ignoring the inexorable change of “steady-state” distributions. These include the understanding of entropy derivatives and links with Fokker-Planck equations. But to us “coarse-graining” appears to be no more than an arbitrary choice, not a necessity.

Though simple, this Baker Map nicely illustrates the puzzle of irreversibility: a time-reversible rule generates a time series of points with irreversible characteristics, a shrinking phase volume, and an ever-increasing probability density, both for a “stationary” dynamics. A variety of maps has been introduced and studied, though only recently has the importance of time-reversibility to their relevance been stressed.¹⁰ Maps can be concatenated into a chain,^{20,21} replacing the solitary Baker by a mass-production “Boulangerie.” The system boundaries, at the two ends of such a chain, can be absorbing, reflecting, or have defined fluxes. Invariably, multifractal phase-space structures, obeying the expected Green-Kubo relations, for near-equilibrium conditions, result.²²

So far we know of no publications, using maps, in which the number of degrees of freedom is increased in more than a single direction, or in which more than a single quantity is conserved (caricaturing mass, momentum, or energy conservation). But there are many potentially interesting possibilities along the continuum separating the conventional Baker Map from state-of-the-art finite-difference or finite-element solutions of the continuum equations. It is still possible that maps are too simple to reveal much about the nonlinear interactions of many particles. Let us proceed to a one-body continuous flow, the Galton Board, which can readily be extended to the many-body case.

III. TIME-REVERSIBLE DISSIPATIVE GALTON BOARD

In 1873 Sir Francis Galton (1822-1911) used his probability demonstrator, the original “Galton Board,” which generated the binomial and Gaussian distributions, by following the progress of an ensemble of moving particles through a periodic array of scatterers.²³ This same idea can be represented computationally as is shown in Fig. 2, where the dynamics of an ensemble, in the full Galton Board, can

be faithfully represented by the time-averaged motion of a single particle in a single unit cell. Five different methods have been used to extract, or to nullify, the influence of the kinetic energy, gained from the field, on the dynamics. Three involve damping: (i) from a pervasive viscous fluid,²⁴ (ii) from inelastic scattering,²⁵ or (iii) from deterministic thermostats.^{9,26} Two others have been used, (iv) time scaling according to a specified function of the coordinates or momenta,²⁷ and (v) field scaling.²⁸ The last three methods produce isomorphic trajectories. With an exponential dependence of the field on the particle coordinate, the particle’s potential energy can maintain a fixed ratio to the kinetic energy, resulting in a dynamic stationary state, in configuration space, but with an exponentially increasing extension in momentum space. All five of the approaches just outlined lead to similar fractal phase-space structures, and to identical transport behavior in the weak-field limit.

Though they are derived from conservative Hamiltonian mechanics, the trajectories generated by time-scaling or field-scaling are isomorphic, meaning “having the same shape,” the same dependence of y on x , to those generated by constant-field thermostated mechanics, “isokinetic mechanics,” in which kinetic energy is extracted from the moving particle by thermostat forces linear in the momentum:

$$\dot{x} = p_x/m, \quad \dot{y} = p_y/m, \quad \dot{p}_x = F_x + E - \zeta p_x,$$

$$\dot{p}_y = F_y - \zeta p_y.$$

Here the forces F describe the interaction of a moving particle with a scatterer (a hard disk interaction in the simplest case) while E is the external field, driving the motion in the x direction. The isokinetic “friction coefficient” ζ is chosen to make the kinetic energy of the moving particle constant:

$$\zeta \equiv [F \cdot p + E p_x]/p^2.$$

In 1986 Bill Moran discovered the multifractal nature of the Galton Board trajectories as well as the complex nature of the motion at very high field strengths.⁹ Soon it became clear that the repeller-attractor pair structure, characteristic of the Board, was shared by most time-reversible nonequilibrium stationary states. The Galton-Board model became a paradigm for irreversibility⁸ because it is the simplest flow to exhibit all the generic features associated with chaotic irreversibility: (i) time-reversible dynamics, (ii) multifractal phase-space structure, including a repeller-attractor pair, (iii) ergodicity, and (iv) overall dissipation, with the paradoxical feature that the “stationary” dynamics continually shrinks the comoving phase volume, while continuing to visit all points in the allowed volume.

The simple two-dimensional “Poincaré section” of the “Galton Board problem” is easy to visualize. This section is a projection of the motion onto a simpler space describing the geometry of the collisions. Two sample sections, an attractor and a repeller, both at a relatively strong field, appear in Fig. 3. So far no three-dimensional continuous ergodic flow, free of singularities and periodicities, has been found to illustrate all these same four features just listed above (reversible repeller-attractor pair with ergodic dissipation). In four dimensions, the thermostated oscillator, with control of

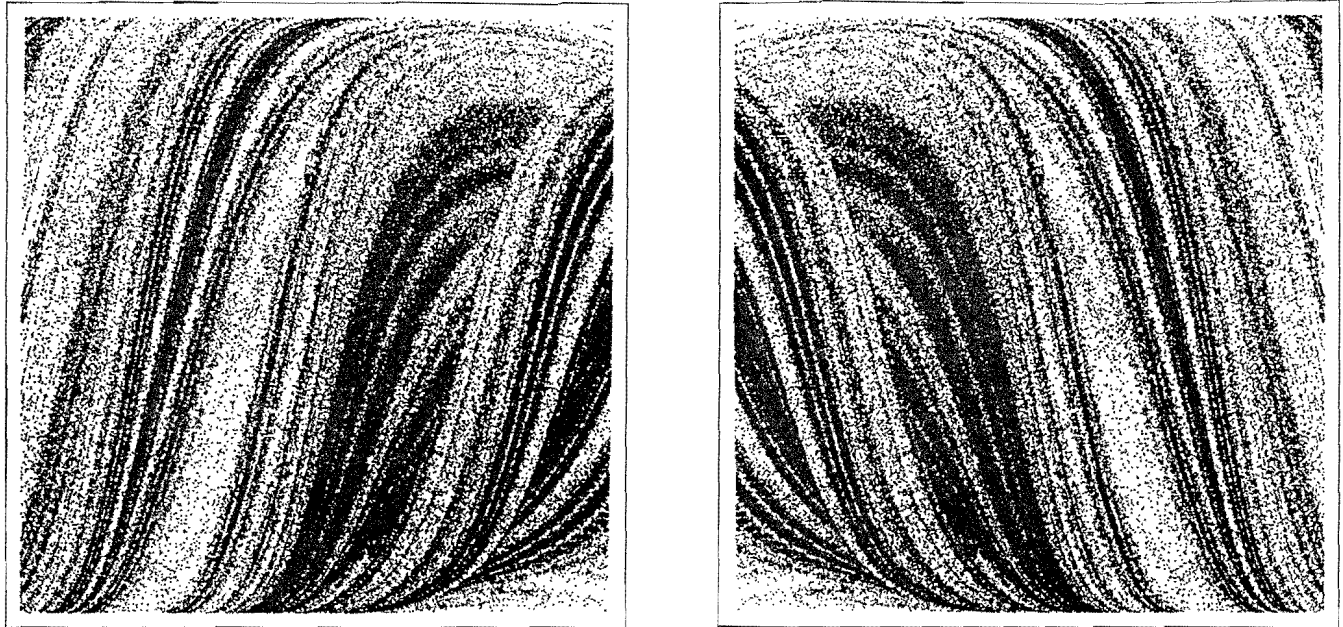


FIG. 3. Poincaré sections, describing the 200 000 collisions, both forward in time, giving the "attractor," shown at the left, and backward, giving the "repellor," shown at the right, for a field strength of $3p^2/(m\sigma)$, where σ is the scatterer diameter. Individual collisions are represented as dots in the section. The abscissa is the angle $0 \leq \alpha \leq \pi$ and the ordinate is $-1 \leq \sin\beta \leq +1$. See Fig. 2. Note that the repellor is the exact mirror image of the attractor.

both the second moment, through ζ , and the fourth moment, through ξ , is the simplest continuous example¹⁰ which avoids the complexities of singularities and periodic boundaries:

$$\begin{aligned} \dot{q} &= p, & \dot{p} &= -q - \zeta p - \xi p^3, & \dot{\zeta} &= p^2 - T, \\ \dot{\xi} &= p^4 - 3p^2. \end{aligned}$$

If the temperature T is chosen to vary with q , $T(q) \equiv 1 + \epsilon \tanh(q/h)$, for instance, then, for reasonable values of ϵ and h , a multifractal ergodic repellor-attractor pair structure develops in the four-dimensional space. In the "equilibrium" nondissipative case, $\epsilon = 0$, the motion reproduces the analytic solution of Liouville's flow equation:²⁹

$$\begin{aligned} \partial f / \partial t &\equiv -\partial(f\dot{q}) / \partial q - \partial(f\dot{p}) / \partial p - \partial(f\dot{\zeta}) / \partial \zeta - \partial(f\dot{\xi}) / \partial \xi, \\ \partial f / \partial t &\equiv 0 \leftrightarrow f(q, p, \zeta, \xi) = e^{-(q^2 + p^2 + \zeta^2 + \xi^2)/2}. \end{aligned}$$

It would be useful to find a three-dimensional mapping analogous to a Poincaré section of this simple set of four equations.

IV. TIME-REVERSIBLE DISSIPATIVE MANY-BODY COLOR CONDUCTIVITY

The Galton Board problem is isomorphic to a two-body periodic problem,³⁰ with one of the two particles, at r with velocity v , accelerated upward, while the second particle, at $-r$ with $-v$, is accelerated downward. This two-body problem generalizes naturally to the two-species many-body "Color Conductivity" problem indicated in Fig. 4, with the field-dependent equations of motion:

$$\begin{aligned} \dot{x} &= p_x/m, & \dot{y} &= p_y/m, & \dot{p}_x &= F_x \pm E - \zeta p_x, \\ \dot{p}_y &= F_y - \zeta p_y, & \dot{\zeta} &= \sum [F \cdot p \pm E p_x] / \sum p^2. \end{aligned}$$

Again, a friction coefficient ζ has been chosen to keep the kinetic energy constant.

Figure 4 illustrates color conductivity in a form suited to thermodynamic analysis. The system, $N/2$ gray particles and $N/2$ black ones, is bathed in a heat reservoir, at temperature T , with such a large heat capacity that the temperature never varies. The heat reservoir could be further visualized as a (nearly) ideal gas of (nearly) massless particles colliding with the system particles in such a way as to force a thermal equilibrium between the thermometer and the system.³¹ The rate at which the system's phase-space volume contracts, according to Liouville's theorem:

$$\begin{aligned} d \ln \Omega / dt &\equiv -d \ln f / dt = \sum (\partial \dot{x} / \partial x) + (\partial \dot{y} / \partial y) + (\partial \dot{p}_x / \partial p_x) \\ &+ (\partial \dot{p}_y / \partial p_y) \equiv -2N\zeta, \end{aligned}$$

is also identical to the rate at which the external entropy S^e of the pervasive heat reservoir increases,

$$-d \ln \Omega / dt \equiv d \ln f / dt = \dot{S}^e / k = -\dot{W} / kT = -\dot{Q} / kT.$$

This relationship holds instantaneously, so that \dot{S}^e , \dot{W} , and \dot{Q} can have either sign. Because $-k \langle d \ln f / dt \rangle$ corresponds also to the time-rate-of-change of Gibbs' system entropy, which decreases, on average, some feel it necessary to ignore the presence of a thermostat and to discuss instead "entropy production," as a property of the system.^{18,19} To us, this emphasis on an ill-defined system entropy, rather than the

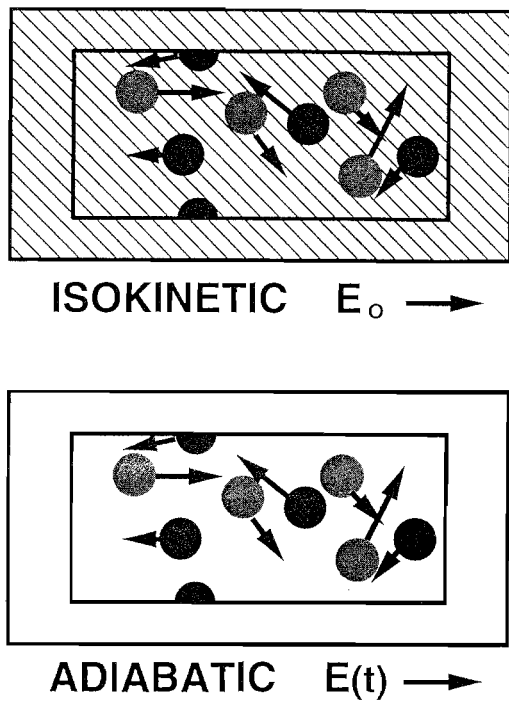


FIG. 4. Thermodynamic views of isokinetic constant-field and adiabatic scaled-field color conductivity simulations. In both cases the external field accelerates gray particles toward the right and black particles to the left. The isokinetic constant-field simulation incorporates a pervasive heat bath, indicated by diagonal stripes, which keeps the system kinetic energy constant. The simulations are isomorphic, with corresponding particles in the two system types tracing out identical $\{x, y\}$ trajectories, so that the comoving ratio, $\ln[f(t)/f_{ideal}]$ is exactly the same for the two dynamics, where f_{ideal} refers to an ideal gas with the same kinetic energy and density.

well-defined entropy of the surroundings, is an arbitrary choice, not a necessity. On a time-averaged dynamical basis only the sign consistent with the macroscopic second law of thermodynamics is also consistent with microscopic dynamical stability, so that $\langle \dot{S}^e/k \rangle > 0$.⁵

The thermostated dynamics just described has an isomorphic twin, with exactly the same particle trajectories $\{y(x)\}$, but with adiabatic equations of motion. Dettmann and Morriss have described a variety of ways to construct corresponding systems obeying fully classical, Hamiltonian and Lagrangian mechanics, without thermostats ($\zeta=0$).^{32,33} Choquard described his independent discovery of some of these same systems in his lecture at this meeting. One of the simplest ways is to impose a special time-dependent field $E(t)$. For finite N it is necessary that the field increase in strict proportion to the kinetic energy, $E(t)/E_0 \equiv K(t)/K_0$. In the large-system limit, which computer simulations indicate is well-behaved, with both finite conductivity and finite Lyapunov exponents,¹³ this scaling takes on a particularly simple form for hard disks or hard spheres:²⁷

$$E(t) = E_0 / [1 - (t/\tau)]^2,$$

where the characteristic time τ corresponds to the time required for the original field, E_0 , to dissipate an energy of order NkT_0 . Similar approaches can be constructed for the study of viscous flows and heat flows.²⁷ It should be stressed that these isomorphisms are not at all limited to the linear-

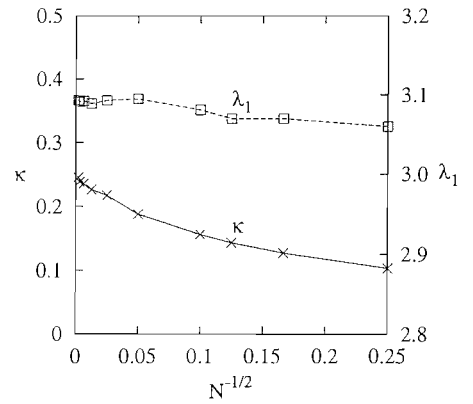


FIG. 5. Number-dependence of the largest Lyapunov exponent, λ_1 , and color conductivity, κ , for two-dimensional particles with a soft repulsive potential. The data in Ref. 13 suggest deviations of order $N^{-1/2}$ from well-defined large-system limiting values.

response Green-Kubo régime. The fully nonlinear, but thermostated, response has an exact analog, multifractal structures and all, in classical mechanics, without thermostats.

In this problem, as well as single-species analogs for the shear and bulk viscosities, and heat conductivity, the weak-field transport coefficient can be shown to reproduce exactly the Gibbs-ensemble predictions of linear-response theory. It appears that the color conductivity, $\kappa \equiv \langle \pm v/E \rangle$, depends smoothly on system size, extrapolating to a well defined, but field-dependent limit, as the number of particles is increased. See Fig. 5.

A similar result holds for the largest Lyapunov exponent λ_1 , which is a measure of the long-time tendency for two nearby trajectories to separate:

$$\begin{aligned} \left\langle \left(\frac{d}{dt} \right) \ln \sum \delta q^2 \right\rangle &\equiv \left\langle \left(\frac{d}{dt} \right) \ln \sum \delta p^2 \right\rangle \\ &\equiv \left\langle \left(\frac{d}{dt} \right) \ln \sum (\delta q^2 + \delta p^2) \right\rangle \\ &\equiv 2\lambda_1. \end{aligned}$$

For exponential separation, the coordinate-space, momentum-space, and phase-space descriptions all give the same Lyapunov exponent. See Fig. 5. The exponential separation rate which characterizes "Lyapunov instability," has some interesting links to macroscopic physics. The largest components of the vector separating the two trajectories lie mainly in a subspace of contiguous particles, as is shown in Fig. 6. A macroscopic explanation for these simple structures, reported on for the first time here, is still missing.

V. DISCUSSION, EMPHASIZING FUTURE DEVELOPMENTS

The three problems outlined here all illustrate (but do not explain) the link between chaotic time-reversible dynamics and irreversible macroscopic behavior. Microstates violating the second law of thermodynamics have probability zero, corresponding to the multifractal nature of the repeller, while the corresponding, and geometrically similar, strange-attractor states attract the flow. The rate at which phase vol-

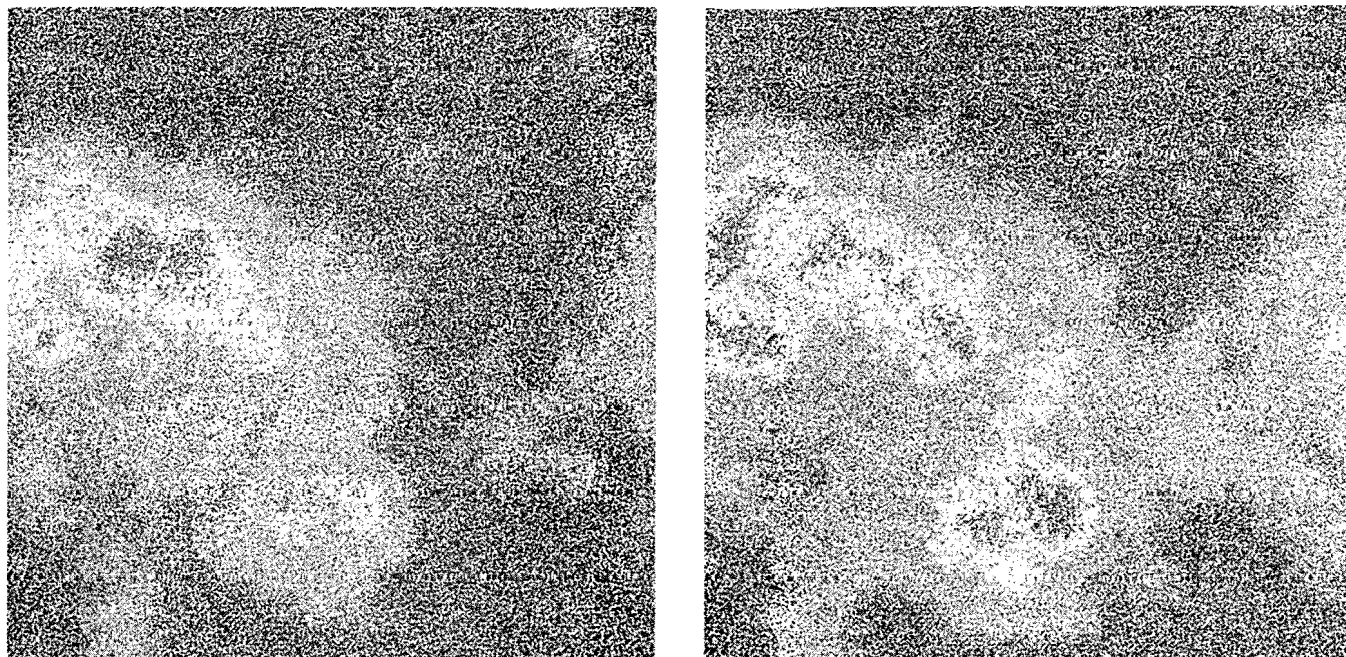


FIG. 6. Typical modes associated with the two largest Lyapunov exponents, λ_1 , shown at the left, and λ_2 , shown at the right, in a color conductivity simulation with 102 400 particles. In the somewhat more-localized mode, at the left, about 1500 particles, with squared offset vectors of 10^{-6} or more, are emphasized. Nine of these particles have contributions exceeding 10^{-2} . In the second-largest mode, shown to the right, the largest squared offset vector is about 10^{-3} . Altogether about 1900 particles make contributions greater than 10^{-6} . Though the figure illustrates the vectors in configuration space, the corresponding vectors in momentum space, or in phase space, look very similar.

ume collapses to the attractor is exactly equivalent to the rate of external entropy increase and to the rate of Gibbs' entropy decrease, $\dot{S}^e/k = -\dot{S}_{\text{Gibbs}}/k = -d\ln\otimes/dt$.

The multifractal structure is the key to understanding the coexistence of time reversibility and macroscopic irreversible dissipation. It is not at all accidental that the same kind of fractal structures appear in the simple chains of maps studied by Breymann, Gaspard, Tasaki, Tél, and Vollmer and found to give identical linear-response conductivities for a variety of boundary conditions. These models have an interesting connection to Fokker-Planck equations.³⁴ Multifractal phase-space objects are also found in the "Escape-Rate" formalism of Gaspard and Nicolis,³⁵ where the fractals then reflect the rarity of equilibrium states constrained to mimic particular nonequilibrium constraints, but with strictly Hamiltonian mechanics.

The focus at Budapest, "Chaos and Irreversibility," clearly revealed two complementary descriptions of nonequilibrium systems: dynamic trajectories, obeying ordinary differential equations, or evolving phase-space distributions, obeying partial differential equations. The dynamic approach seems to us much simpler, in many ways. It corresponds more closely to laboratory experiments, to practical simulation techniques, and its mathematics is simpler. It should not be discounted that the fractal structures which complicate a phase-space distribution-function analysis were actually discovered as time series generated by a simple dynamics. The "irreversible entropy production" of the distribution-function approach, as formulated by its adherents, is identical to the external entropy increase of a heat reservoir (see again Fig. 4) in interaction with a single dynamical system. It

appears that the two approaches are in full agreement, at least insofar as linear irreversible thermodynamics is concerned. Any further advances, toward understanding truly nonlinear processes, await further results from dynamics, not from ensemble theory.

It is particularly interesting that diffusive, viscous, and conducting flows can be simulated with both non-Hamiltonian and Hamiltonian, or Lagrangian, equations of motion, with exactly isomorphic trajectories.²⁷ It is possible to show that the fraction of the available space occupied by the attractor is the same in both cases. In the thermostated case phase volume shrinks, relative to the total, as time passes. In the Hamiltonian and Lagrangian cases the driven system heats up, and the constant phase volume occupies a declining fraction of the increasing "accessible" phase space.

Some of those who initially doubted the fractal explanation of the link between chaos and irreversibility^{15,36} have by now constructed their own convincing examples,³⁷ which should quell the concerns of the unconvinced. In less than a generation, Boltzmann's original explanation of the link between chaos and irreversibility, limited as it was, has been generalized to apply to a wide range of systems, stationary and periodic, dense and dilute, fluid and solid.

Computer simulations of shear flows³⁸ show that nonlinear effects are typically very small. Even in the strongest shock waves³⁹ the effects due to nonlinearity are no more than 30%. Nevertheless, there remains a need to leave the naive models behind, to go beyond Green-Kubo linear response theory and the results of linear irreversible thermodynamics.^{40,41} Shock waves, with their strongly non-

equilibrium structures enclosed by equilibrium boundary conditions, are probably the simplest choice. Nonequilibrium phase transitions likewise call for the study of a transition region maintained by boundary fluxes. Both problems are well within current computational abilities. A study of noise, as seen in dynamical simulations, should prove fruitful in providing increased understanding of the difference between the microscopic and macroscopic descriptions of nonequilibrium processes.¹⁹ Likewise, there is a possibility that efforts to improve upon the predictions of the Central Limit Theorem⁴² will pay off, giving estimates of nonequilibrium fluctuations far from equilibrium. Though it is difficult to design fully classical experiments, the challenge of devising experimental confirmations of the complex multifractal structures found with simulations, and with theoretical analyses, remains.

ACKNOWLEDGMENTS

We have discussed reversibility with a number of colleagues, and have profited particularly from recent conversations with Aurel Bulgac, Christoph Dellago, Carl Dettmann, Denis Evans, Brad Holian, Carol Hoover, Dimitri Kusnezov, Joel Lebowitz, Michel Mareschal, Gregoire Nicolis, and Tamás Tél. The novel eigenvector plots appearing in Fig. 6 were generated with the help of Kevin Boercker.¹³ Work at the Lawrence Livermore National Laboratory was performed under the auspices of the University of California, through Department of Energy Contract W-7405-eng-48. Work at the University of Vienna was supported by the Fonds zur Förderung der wissenschaftlichen Forschung, Grant P11428-PHY.

¹B. J. Alder and T. E. Wainwright, *Sci. Am.* **201**, 113 (1959).

²A. W. Lees and S. F. Edwards, *J. Phys. C* **5**, 1921 (1972).

³W. T. Ashurst and W. G. Hoover, *Phys. Rev. Lett.* **31**, 206 (1973); *Phys. Rev. A* **11**, 658 (1975).

⁴B. L. Holian, W. G. Hoover, and H. A. Posch, *Phys. Rev. Lett.* **59**, 10 (1987).

⁵W. G. Hoover, H. A. Posch, B. L. Holian, M. J. Gillan, M. Mareschal, and C. M. Massobrio, *Mol. Simul.* **1**, 79 (1987).

⁶B. L. Holian, P. S. Lomdahl, and S. J. Zhou, *Physica A* **240**, 340 (1997).

⁷J. Bricmont, *Phys. Mag.* **17**, 159 (1995); see Sec. 3.

⁸N. I. Chernov, G. L. Eyink, J. L. Lebowitz, and Y. G. Sinai, *Phys. Rev. Lett.* **70**, 2209 (1993).

⁹B. Moran, W. G. Hoover, and S. Bestiale, *J. Stat. Phys.* **48**, 709 (1987).

¹⁰Wm. G. Hoover, O. Kum, and H. A. Posch, *Phys. Rev. E* **53**, 2123 (1996).

¹¹W. G. Hoover, C. G. Tull, and H. A. Posch, *Phys. Lett. A* **131**, 211 (1988).

¹²H. A. Posch, Ch. Dellago, W. G. Hoover, and O. Kum, in *Pioneering Ideas for the Physical and Chemical Sciences*, edited by W. Fleischhacker and T. Schönfeld (Plenum, New York, 1997), pp. 233–248.

¹³W. G. Hoover, K. Boercker, and H. A. Posch, *Phys. Rev. E* **57**, 3911 (1998).

¹⁴J. D. Farmer, E. Ott, and J. A. Yorke, *Physica D* **7**, 153 (1983).

¹⁵See the discussions in *Microscopic Simulations of Complex Hydrodynamic Phenomena*, edited by M. Mareschal and B. L. Holian, Vol. 292, NATO ASI Series in Physics (Plenum, New York, 1992).

¹⁶D. Levesque and L. Verlet, *J. Stat. Phys.* **72**, 519 (1993).

¹⁷O. Kum and W. G. Hoover, *J. Stat. Phys.* **76**, 1075 (1994).

¹⁸P. Gaspard, *J. Stat. Phys.* **88**, 1215 (1997).

¹⁹G. Nicolis and D. Daems, *J. Phys. Chem.* **100**, 19187 (1996).

²⁰S. Tasaki and P. Gaspard, *J. Stat. Phys.* **81**, 935 (1995).

²¹J. Vollmer, T. Tél, and W. Breymann, *Phys. Rev. Lett.* **79**, 2759 (1997).

²²W. Breymann, T. Tél, and J. Vollmer, *Phys. Rev. Lett.* **77**, 2945 (1996).

²³K. Pearson, *The Life, Letters and Labours of Francis Galton*, Vol. III (Cambridge University Press, Cambridge, England, 1930).

²⁴W. G. Hoover and B. Moran, *Chaos* **2**, 599 (1992).

²⁵A. Luc and H. Brenner, *Phys. Rev. E* **47**, 3128 (1993).

²⁶W. G. Hoover and B. Moran, *Phys. Rev. A* **40**, 5319 (1989).

²⁷Wm. G. Hoover, *Phys. Lett. A* **235**, 357 (1997).

²⁸W. G. Hoover, B. Moran, C. G. Hoover, and W. J. Evans, *Phys. Lett. A* **133**, 114 (1988).

²⁹L. Andrey, *Phys. Lett. A* **111**, 45 (1985); **114**, 183 (1986).

³⁰A. J. C. Ladd and W. G. Hoover, *J. Stat. Phys.* **38**, 973 (1985).

³¹W. G. Hoover, B. L. Holian, and H. A. Posch, *Phys. Rev. E* **48**, 3196 (1993).

³²C. P. Dettmann and G. P. Morriss, *Phys. Rev. E* **54**, 2495 (1996).

³³C. P. Dettmann and G. P. Morriss, *Phys. Rev. E* **55**, 3693 (1997).

³⁴T. Tél, J. Vollmer, and W. Breymann, *Europhys. Lett.* **35**, 659 (1996).

³⁵P. Gaspard and G. Nicolis, *Phys. Rev. Lett.* **65**, 1693 (1990).

³⁶M. Mareschal, *Adv. Chem. Phys.* **100**, 317 (1997).

³⁷N. L. Chernov and J. L. Lebowitz, *Phys. Rev. Lett.* **75**, 2831 (1995).

³⁸S. Y. Liem, D. Brown, and J. H. R. Clarke, *Phys. Rev. A* **45**, 3706 (1992).

³⁹B. L. Holian, W. G. Hoover, B. Moran, and G. K. Straub, *Phys. Rev. A* **22**, 2798 (1980).

⁴⁰W. G. Hoover, *Computational Statistical Mechanics* (Elsevier, Amsterdam, 1991).

⁴¹D. J. Evans and G. P. Morriss, *Statistical Mechanics of Nonequilibrium Liquids* (Academic, New York, 1990).

⁴²D. J. Evans, E. G. D. Cohen, and G. P. Morriss, *Phys. Rev. Lett.* **71**, 2401 (1993).